Density Functional Theory Calculation of Molecular Structure and Vibrational Spectra of Dibenzothiophene in the Ground and the Lowest Triplet State

Sang Yeon Lee*

Department of Industrial Chemistry, Kyungpook National University, Taegu, 702-701, S. Korea

Received: March 15, 2001; In Final Form: June 11, 2001

The molecular geometries and harmonic vibrational frequencies of the ground and the lowest triplet state of dibenzothiophene have been calculated using the Becke-3-Lee−Yang−Parr (B3LYP) density functional methods with the 6-31G* basis set. A structural change occurs from a benzene-like to a planar, quinone-like form upon the excitation to the first excited state. Scaled vibrational frequencies for the ground state obtained from the B3LYP calculation show good agreement with experiment. On the basis of the calculated and experimental vibrational frequencies, a few vibrational fundamentals for both states are newly assigned and the spectral position of some missing lines are predicted.

I. Introduction

Dibenzothiophene (DBT) and its derivatives have been studied experimentally and theoretically to investigate their molecular structure and spectroscopic properties.[1−11] A complete vibrational analysis for DBT in the ground state would be very useful for the interpretation of the vibronic structures in the absorption and fluorescence spectra. Bree and Zwarich (BZ)[9] employed polarized infrared and Raman spectra of a single crystal to obtain a symmetry determination of the observed vibrational frequencies of DBT and perdeuterated DBT (DBT-d_8) in the ground state. However, their selection of fundamental frequencies from the complicated infrared and Raman spectra is not complete, and has some ambiguity, since the selection was done based on the assumption that the fundamental modes show the most intense bands in the spectra and that the oriented gas model provides a reliable qualitative guide to the polarization characteristics. In addition, there are some missing assignments for the a_2 modes due to the forbidden infrared selection rule and to the very weak Raman scattering activities of these modes. Recently, Buntinx and Poizat(BP) analyzed the transient resonance Raman spectra of DBT in the first-excited triplet state and suggested that DBT in the first-excited triplet state takes a quinone-like structure.[11] It is necessary to perform a reliable theoretical vibrational calculation for DBT in the ground and the first triplet state in order to predict the vibrational frequencies of a_2 modes that are unobserved in the vibtational spectra, clarify the remained ambiguities in the assignment of fundamentals of DBT in the ground state, and assign the peaks appearing in the resonance Raman spectra of DBT in the lowest triplet state.

Density functional theory calculations[12−24] have been reported to provide excellent vibrational frequencies of organic compounds if the calculated frequencies are scaled to compensate for basis set deficiencies, anharmonicity, and the approximate treatment of electron correlation. Some studies indicate that the vibrational frequencies and intensities from density functional calculations are better than those obtained from second-order Möller−Plesset perturbation theory.[24] Baker, Jarzecki, and Pulay[25] calculated the vibrational spectra of sixty molecules using the Becke-3-Lee−Yang−Parr (B3LYP)[26] functionals with the 6-31G* basis set and with direct scaling in which the calculated force-constant matrix in Cartesian coordinates is transformed to redundant-internal coordinates and then the resulting force constants are scaled. In their work, they calculated vibrational frequencies for a training set of thirty molecules whose experimental vibrational frequencies are well assigned, and derived transferable scaling factors by using the least-squares procedure. The scaling factors were successfully applied to a test set of thirty other molecules. The direct scaling procedure shows an average error of less than 8.5 cm^{-1}.

By using the B3LYP/6-31G* method, we have calculated the vibrational frequencies of DBT in the ground state to distinguish the fundamentals from the many experimental vibrational frequencies and to predict the spectral positions of the missing lines. Furthermore, the same theoretical vibrational analysis is performed for the DBT in the first-excited triplet state to assign the peaks observed in the transient Raman spectra and investigate BP's suggestion that the DBT in the first-excited state takes a quinone-like structure.

II. Calculations

The molecular structures of DBT in the ground and the first-excited triplet state are optimized at the B3LYP/6-31G* level. The unrestricted B3LYP method is employed in the geometry optimization for DBF in the triplet state. The harmonic vibrational frequencies for the DBT in the ground and the lowest triplet state are calculated with the B3LYP with the 6-31G* basis. All the calculations for geometry optimization and harmonic vibrational frequencies are performed by using the Gaussian 98 program.[27]

The calculated vibrational frequencies are scaled by employing multiple scaling factors. The scaling procedure employed in this work is similar to the direct scaling technique developed by Baker and co-workers.[25] This procedure is now summarized. The calculated force constant matrix in Cartesian coordinates

* Corresponding author's address. Prof. Sang Yeon Lee, Department of Industrial Chemistry, Kyungpook National University, Taegu, 702-701, S. Korea. Tel: + 82-950-5583. Fax: + 82-950-6594. E-mail: sanglee@knu.ac.kr.

10.1021/jp010991i CCC: $20.00
Published on Web 08/02/2001

is transformed into the corresponding one in redundant internal coordinates. Then the resulting force constant is scaled by using

$$F_{ij}^{\text{scal}} = \sqrt{s_i s_j} F_{ij}^{\text{int}} \quad (1)$$

where s_i and s_j are scaling factors for the internal coordinate i and j, respectively. The scaled-force constant-matrix is diagonalized to provide the vibrational frequencies. The scaling factors are optimized by using a least-squares method, that is, by minimizing

$$\chi^2(s) = \sum_i \left(\frac{\nu_i^{\text{scaled}}(s) - \nu_i^{\text{exp}}}{\nu_i^{\text{exp}}} \right)^2 \omega_i \quad (2)$$

where ω_i is the weighting factor for ith mode—either one or zero.

It should be noted that, in this work, redundant internal coordinates are employed in the transformation of force-constant matrix instead of nonredundant internal coordinates because—as reported by Baker and co-workers[25]—the use of redundant internal coordinates is more flexible than nonredundant internal coordinates in the scaled, quantum-mechanical, force-field calculations. The scalings are carried out by using a modified version of the redong program.[28]

III. Results and Discussion

A. Molecular Geometry. The DBT ground state has C_{2v} symmetry. The optimized geometric parameters at the B3LYP/6-31G* level are listed in Table 1 with the experimental geometry obtained from X-ray diffraction.[6] The atomic numbering in DBT is shown in Figure 1. The optimized bond lengths are in good agreement with the corresponding experimental bond lengths. The bond angles from the calculation and the experiment are in good accord with each other.

The molecular structure optimized at the B3LYP level for the first-excited triplet state is also included in Table 1. The calculated geometry of the lowest triplet state retains the ground state's planar C_{2v} conformation. As suggested by Bree and Zwarich, this state has an A_1 spatial symmetry.[5] Upon the excitation to the first-excited triplet state, the C_1-C_2, C_3-C_4, C_4-C_{11}, and $C_{10}-C_{11}$ bonds elongate by 0.025, 0.017, 0.018, and 0.028 Å, respectively, while the C_1-C_{10}, S_9-C_{10}, and $C_{11}-C_{12}$ bonds become shorter by 0.006, 0.036, and 0.036 Å, respectively. This geometrical change is consistent with BP's suggestion—based on the analysis of the transient Raman spectra—that the structure changes from a benzene-like to a quinone-like form when going from the ground to the lowest triplet state.

B. Vibrational Frequencies of Dibenzothiophene and Perdeuterated Dibenzothiophene (DBT-d_8) in the Ground-State. DBT in the ground state has 57 fundamentals with the various symmetries of 20 a_1 + 9 a_2 + 9 b_1 + 19 b_2. According to the group theoretical analysis of the selection rules for DBT in infrared and Raman spectra, all the symmetric modes are Raman active but only the a_1, b_1, and b_2 symmetric modes are infrared active. The scaled vibrational frequencies, infrared intensities, Raman activities, and depolarization ratios—obtained from the B3LYP calculation for DBT and DBT-d_8—are listed in Table 2. In this work, scaling factors are derived in two steps. In the first step, the scaling factors are derived from the vibrational analysis for benzene and thiophene and are directly applied to DBT and DBT-d_8 in the ground state to predict and assign the vibrational frequencies. The root-mean-square (rms) deviations of scaling vibrational frequencies from the experimental ones are 15.1 and 9.4 cm^{-1} for DBT and DBT-d_8, respectively. In the second step, the scaling factors are optimized for DBT-d_8 using the vibrational data assigned at the first step because the rms deviation for DBT-d_8 is smaller than it is for DBT in the previous step. A weighting factor of zero for some uncertain fundamental modes is used in the optimization. The optimized scaling factors are applied to DBT. The rms deviations for DBT and DBT-d_8 are 12.7 and 4.5 cm^{-1}, respectively. The rms deviation for DBT becomes 7.7 cm^{-1} if CH stretching modes are not considered. This scaled vibrational frequencies are listed in Table 2 and are in excellent agreement with experimental values. The experimental vibrational frequencies reported by BZ are also included for comparison. The frequencies noted in **boldface** under the experiment column are newly assigned to fundamental vibrational frequencies. The frequencies in *italics* are tentatively assigned to fundamental modes based

TABLE 1: Optimized and Experimental Geometries of Dibenzothiophene in the Ground and the Lowest Triplet State

	ground state		triplet state
parameter[a]	B3LYP	exp.[b]	B3LYP
$R(C_1-C_{10})$	1.397	1.386	1.391
$R(C_1-C_2)$	1.392	1.384	1.417
$R(C_2-C_3)$	1.404	1.385	1.400
$R(C_3-C_4)$	1.390	1.370	1.407
$R(C_4-C_{11})$	1.403	1.392	1.421
$R(S_9-C_{10})$	1.768	1.74	1.748
$R(C_{10}-C_{11})$	1.413	1.409	1.441
$R(C_{11}-C_{12})$	1.455	1.441	1.419
$R(C_1-H_{14})$	1.086		1.086
$R(C_2-H_{15})$	1.087		1.084
$R(C_3-H_{16})$	1.086		1.088
$R(C_4-H_{17})$	1.087		1.085
$\angle(C_1-C_{10}-C_{11})$	121.6	121.6	124.2
$\angle(C_1-C_{10}-S_9)$	126.0	126.1	125.4
$\angle(C_1-C_2-C_3)$	120.9	121.6	118.4
$\angle(C_2-C_1-C_{10})$	118.5	117.8	118.5
$\angle(C_2-C_3-C_4)$	120.5	120.5	123.2
$\angle(C_3-C_4-C_{11})$	119.9	120.0	119.8
$\angle(C_4-C_{11}-C_{10})$	118.8	118.7	115.9
$\angle(C_4-C_{11}-C_{12})$	129.1	129.4	131.2
$\angle(S_9-C_{10}-C_{11})$	112.4	112.3	110.4
$\angle(C_{10}-C_{11}-C_{12})$	112.2	111.9	112.9
$\angle(C_{10}-S_9-C_{13})$	91.0	91.5	93.3
$\angle(C_2-C_1-H_{14})$	120.7		120.8
$\angle(C_{10}-C_1-H_{14})$	120.8		120.6
$\angle(C_1-C_2-H_{15})$	119.5		120.5
$\angle(C_3-C_2-H_{15})$	119.8		121.1
$\angle(C_4-C_3-H_{16})$	119.8		118.8
$\angle(C_2-C_3-H_{16})$	119.7		118.0
$\angle(C_3-C_4-H_{17})$	120.2		119.8
$\angle(C_{11}-C_4-H_{17})$	120.0		120.4

[a] Bond lengths in angstrom, and angles in degree. [b] Values from an X-ray diffraction experiment; reference 6.

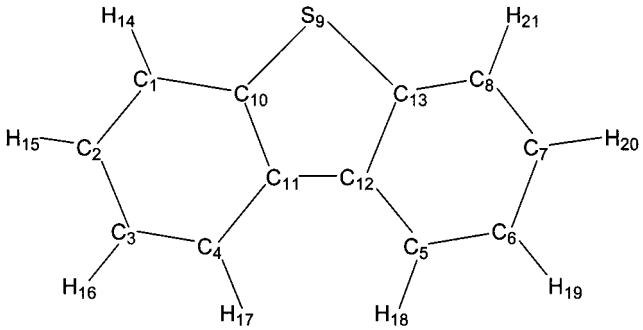

Figure 1. The atomic numbering in dibenzothiophene.

TABLE 2: Comparison of Calculated and Experimental Vibrational Frequencies of Dibenzothiophene(DBT) and Perdeuterated Dibenzothiophene(DBT-d_8) in the Ground State

sym.	DBT					DBT-d_8					approximate
mode	freq[a]	I_{IR}[b]	I_{Raman}[c]	DP[d]	exp.[e]	freq[a]	I_{IR}[b]	I_{Raman}[c]	DP[d]	exp.[e]	mode description[f]
a_1 symmetry											
ν_1	212	0.80	1.15	0.59	218	198	0.72	0.97	0.58	203	ring defm
ν_2	407	2.63	13.33	0.23	410	392	2.38	13.27	0.24	396	ring defm + ip(CH)
ν_3	493	0.15	5.13	0.33	498	485	0.10	5.07	0.33	485	ring defm + ip(CH)
ν_4	708	1.35	19.73	0.11	704	667	1.14	16.02	0.11	665	ring defm + ip(CH)
ν_5	770	0.59	2.72	0.12	771	722	1.70	0.18	0.08	723	ring defm + ip(CH)
ν_6	1017	2.62	61.48	0.14	1027	825	0.06	1.66	0.21	832	ip(CH) + ring defm
ν_7	1065	8.29	12.97	0.34	1072	844	0.32	23.13	0.11	840	ip(CH) + ring defm
ν_8	1130	1.62	50.86	0.17	1137	863	2.38	3.42	0.35	854	ip(CH) + ring defm
ν_9	1156	0.91	1.87	0.63	**1155**	985	0.09	1.77	0.14	**991**	ip(CH) + ring defm
ν_{10}	1224	17.02	61.30	0.32	1236	1060	11.25	72.60	0.21	1057	ip(CH) + ring defm
ν_{11}	1310	0.24	177.10	0.25	1321	1204	5.12	157.20	0.23	1205	ip(CH) + str(CC,CS) + ring defm
ν_{12}	1333	4.07	5.37	0.22	**1334**	1284	6.10	35.90	0.34	1286	ip(CH) + str(CC,CS) + ring defm
ν_{13}	1426	25.68	2.39	0.69	1421	1326	22.16	8.90	0.14	1320	str(CC,CS) + ip(CH) + ring defm
ν_{14}	1488	0.18	77.51	0.29	1480	1430	2.06	108.02	0.27	1421	str(CC,CS) + ip(CH) + ring defm
ν_{15}	1557	0.21	68.42	0.46	1558	1519	0.22	58.82	0.47	1529	str(CC,CS) + ring defm + ip(CH)
ν_{16}	1601	1.14	266.26	0.41	1601	1576	4.17	318.56	0.39	1576	str(CC,CS) + ring defm
ν_{17}	3068	0.04	17.13	0.74	3000	2261	0.09	5.57	0.72	**2267**	str(CH)
ν_{18}	3076	0.47	172.14	0.75	3025	2271	0.05	67.33	0.74	**2270**	str(CH)
ν_{19}	3085	44.88	14.47	0.73	3060	2283	26.35	8.91	0.74	2284	str(CH)
ν_{20}	3094	2.91	638.19	0.12	3065	2293	1.38	257.80	0.12	2294	str(CH)
a_2 symmetry											
ν_1	135	0.00	0.12	0.75	*140*	122	0.00	0.11	0.75	*126*	ring tors
ν_2	275	0.00	7.98	0.75	287	255	0.00	5.75	0.75	261	ring tors
ν_3	436	0.00	0.37	0.75		385	0.00	0.50	0.75	385	ring tors + oop(CH)
ν_4	559	0.00	0.39	0.75	**562**	493	0.00	0.34	0.75		ring tors + oop(CH)
ν_5	730	0.00	3.71	0.75	730	589	0.00	0.21	0.75	586	ring tors + oop(CH)
ν_6	781	0.00	1.13	0.75	768	646	0.00	0.01	0.75	646	oop(CH) + ring tors
ν_7	859	0.00	1.09	0.75		738	0.00	0.16	0.75	747	oop(CH) + ring tors
ν_8	929	0.00	0.87	0.75	938	775	0.00	0.15	0.75	774	oop(CH) + ring tors
ν_9	969	0.00	0.07	0.75		813	0.00	0.71	0.75	-	oop(CH) + ring tors
b_1 symmetry											
ν_1	104	1.03	0.66	0.75	*107*	97	0.98	0.40	0.75	**97**	ring tors
ν_2	224	0.61	2.27	0.75	226	214	0.55	1.43	0.75	217	ring tors
ν_3	419	3.93	0.01	0.75	421	369	6.46	0.00	0.75	369	ring tors + oop(CH)
ν_4	498	1.52	0.36	0.75	497	453	2.14	0.12	0.75	449	ring tors + oop(CH)
ν_5	700	0.49	0.47	0.75	**704**	578	47.25	0.11	0.75	574	ring tors + oop(CH)
ν_6	749	100.20	0.65	0.75	740	629	0.00	1.09	0.75	630	oop(CH) + ring tors
ν_7	855	0.00	7.29	0.75	859	702	0.03	0.32	0.75	**705**	oop(CH) + ring tors
ν_8	928	1.50	0.04	0.75	940	752	1.51	0.01	0.75	759	oop(CH) + ring tors
ν_9	971	0.06	0.02	0.75	973	794	0.01	0.00	0.75	**801**	oop(CH) + ring tors
b_2 symmetry											
ν_1	420	0.37	2.95	0.75	420	407	0.23	1.78	0.75	408	ring defm
ν_2	515	1.16	5.26	0.75	**509**	489	1.28	6.51	0.75	492	ring defm + ip(CH)
ν_3	617	5.19	0.07	0.75	612	595	5.44	0.10	0.75	592	ring defm + ip(CH)
ν_4	710	6.64	3.90	0.75	704	675	5.20	2.38	0.75	670	ring defm + ip(CH)
ν_5	988	0.63	0.91	0.75	**990**	812	1.71	0.37	0.75	**818**	ring defm + ip(CH)
ν_6	1020	15.87	0.17	0.75	1027	837	0.00	1.88	0.75	831	ip(CH) + ring defm
ν_7	1075	10.23	0.86	0.75	1078	848	0.41	6.80	0.75	854	ip(CH) + ring defm
ν_8	1128	1.76	2.75	0.75		961	0.42	0.96	0.75	**965**	ip(CH) + ring defm
ν_9	1157	2.35	8.79	0.75	1171	1017	3.96	1.98	0.75	1017	ip(CH) + ring defm
ν_{10}	1263	0.41	6.08	0.75	1268	1039	23.34	1.63	0.75	1040	ip(CH) + ring defm
ν_{11}	1322	7.97	7.70	0.75	**1314**	1292	17.61	10.64	0.75	1293	ip(CH) + ring defm
ν_{12}	1444	8.65	0.90	0.75	1442	1336	3.48	3.53	0.75	1338	ip(CH) + ring defm
ν_{13}	1473	20.28	2.69	0.75	1462	1371	6.21	4.03	0.75	**1381**	str(CC,CS) + ip(CH) + ring defm
ν_{14}	1576	1.34	10.09	0.75	1566	1544	3.88	8.12	0.75	1542	str(CC,CS) + ring defm
ν_{15}	1588	4.88	14.80	0.75	1590	1565	4.61	11.79	0.75	1564	str(CC,CS) + ring defm
ν_{16}	3066	1.59	51.17	0.75	3025	2261	0.77	19.08	0.75	**2267**	str(CH)
ν_{17}	3074	7.04	12.86	0.75	3055	2270	3.09	15.81	0.75	**2270**	str(CH)
ν_{18}	3084	0.27	161.06	0.75	3055	2283	1.21	59.91	0.75	2283	str(CH)
ν_{19}	3093	52.41	0.16	0.75	3117	2292	27.25	0.09	0.75	2293	str(CH)

[a] Vibrational frequencies in cm^{-1}. [b] Infrared intensities in KM/mol. [c] Raman scattering activities in $Å^4$/AMU. [c] Raman depolarization ratios. [d] Reference 9. [e] Ring defm, ring deformaton; ring tors, ring torsion; str, stretching; oop, out-of-plane bending; ip, in-plane bending.

on the present calculations. Since almost all the vibrational modes are delocalized over the whole molecule, they cannot be ascribed to several local vibrational motions. This is a characteristic feature of cyclic compounds, particularly aromatic compounds. Thus, the modes for DBT are described only approximately in Table 2.

a_1 Symmetry. By using the computational results and the symmetry assigned peaks in infrared and Raman spectra reported

by BZ, we have made a reliable one-to-one correspondence between our fundamentals and the experimental data. The a_1 symmetric fundamental modes of DBT are observed at 218, 410, 498, 704, 771, 1027, 1072, 1137, 1155, 1236, 1321, 1334, 1421, 1480, 1558, 1601, 3040, 3060, 3082, and 3070 cm^{-1}. The peaks observed at 1155 and 1334 cm^{-1} are newly assigned to fundamentals instead of the peaks located at 1203 and 1410 cm^{-1}. The fundamental modes of DBT-d_8 are observed at 203, 396, 485, 665, 723, 832, 840, 854, 991, 1057, 1205, 1286, 1320, 1421, 1529, 1576, 2000, 2267, 2270, 2284, and 2294 cm^{-1}. The peak at 991 cm^{-1} is newly assigned to fundamental modes instead of the peak at 1122 cm^{-1}. These symmetry modes have totally symmetric vibrations. The fundamental modes below 1650 cm^{-1} are in-plane vibrations and consist of planar inter-ring torsion, ring bendings, CC stretchings, and CH bendings. The higher frequencies are from CH stretchings.

a_2 Symmetry. Although these modes are Raman active, their Raman scattering activities are calculated to be relatively weak. Six of the nine fundamentals having a_2 symmetry for DBT are observed at 287, 560, 730, 768, 938, and 968 cm^{-1}. The peak observed at 617 cm^{-1} that was ascribed to a fundamental is shown *not* to be a real fundamental mode. BZ observed a peak at 562 cm^{-1} in Raman spectra of the crystal, but could not determined its symmetry. This peak is assigned to the fourth fundamental. Terada and co-workers[10] observed a peak at 565 cm^{-1} in the phosphorescence spectra and found out its symmetry to be a_2. Their observation supports present assignment for the fourth a_2 fundamental. BZ observed a peak at 970 cm^{-1} in Raman spectra of the crystal and suggested that the symmetry of the peak may be a_1. The peak is probably the ninth a_2 fundamental. The lowest peak having the a_2 symmetry is observed at 171 cm^{-1}, and is in poor agreement with the calculated one that is at 135 cm^{-1}. If the observed peak is assumed to originate from the combination band of the lowest a_2 mode and the lowest totally symmetric crystal mode—observed at 31 cm^{-1}—then the first a_2 mode is expected to be at 140 cm^{-1}. The deduced frequency is then in good accord with the calculated one. Situations similar to this case are found for the assignment of the lowest a_2 and b_1 modes for both DBT and DBT-d_8. When the same recipe is applied to these cases, the deduced frequencies are in good agreement with the corresponding calculated ones. Hence, this assumption seems to be effective. The unobserved third and seventh a_2 fundamentals are predicted to be located at 436 and 859 cm^{-1}, respectively. The third a_2 fundamental seems to overlap with the peak at 438 cm^{-1}, and the ninth a_2 fundamental overlaps with the peak at 970 cm^{-1}. The fundamental modes of DBT-d_8 are observed at 261, 385, 586, 646, 747, and 774 cm^{-1}. The first fundamental mode calculated to be at 122 cm^{-1} is in good agreement with the frequency, 126 cm^{-1}, deduced from the peak observed at 157 cm^{-1}, as mentioned before. The unobserved fourth and ninth modes are predicted to be located at 493 and 813 cm^{-1}, respectively, and are expected to overlap with the peaks at 492 and 818 cm^{-1}, respectively. All symmetry modes below 1000 cm^{-1} consist of inter-ring out-of-plane bending, ring deformations, and CH out-of-plane bendings.

b_1 Symmetry. Seven of the nine fundamentals assigned to the b_1 mode are at 226, 421, 497, 740, 859, 940, and 973 cm^{-1}. The calculated frequency for the first b_1 mode, 104 cm^{-1}, shows good agreement with the frequency, 107 cm^{-1}, and is deduced from the lowest peak having a b_1 symmetry that is found at 138 cm^{-1}. BZ assigned the peak observed at 724 cm^{-1} to the fifth b_1 fundamental, but the calculation predicts it at 700 cm^{-1}. There is a peak at 705 cm^{-1} whose symmetry may be b_2. Perhaps, this peak is the fifth b_1 mode. The fundamental modes of DBT-d_8 are observed at 217, 369, 449, 559, 630, 705, 759, and 801 cm^{-1}. Similarly to the first a_2 mode of DBT, the frequency of 97 cm^{-1}—deduced from the peak observed at 128 cm^{-1}—agrees well with the calculated value of 97 cm^{-1}. The peaks at 574, 705, and 801 cm^{-1} are newly assigned to fundamental modes instead of the peaks at 559, 618, and 907 cm^{-1}. All symmetry modes below 1000 cm^{-1} consist of inter-ring out-of-plane bending, ring deformations, and CH out-of-plane bendings.

TABLE 3: Comparison of Calculated and Experimental Vibrational Frequencies of Dibenzothiophene in the Lowest Triplet State

	ground state		triplet state		
symmetry	calc.[a]	exp.[b]	calc.[a]	exp.[c]	exp.[d]
a_1 symmetry					
ν_1	205	218	199		
ν_2	396	410	392		
ν_3	480	498	471		
ν_4	689	704	671		
ν_5	753	771	738		
ν_6	1018	1027	991	977	977
ν_7	1045	1072	1020		
ν_8	1115	1137	1077		1079
ν_9	1151	1155	1087		
ν_{10}	1214	1236	1198		
ν_{11}	1299	1321	1275		
ν_{12}	1312	1334	1316	1330	1330
ν_{13}	1417	1421	1394		
ν_{14}	1465	1480	1438	1445	1445
ν_{15}	1556	1558	1482		
ν_{16}	1594	1601	1575	1531	
ν_{17}	3070	3000	3064		
ν_{18}	3078	3025	3080		
ν_{19}	3087	3060	3091		
ν_{20}	3096	3065	3111		

[a] Vibrational frequencies in cm^{-1}; frequencies are scaled by a factor of 0.963. [b] Reference 9. [c] Reference 11. [d] Present assignments.

b_2 Symmetry. Nineteen fundamentals attributable to the b_2 mode are observed at 420, 505, 612, 704, 990, 1027, 1078, 1171, 1268, 1321, 1442, 1462, 1566, 1590, 3025, 3055, 3055, and 3117 cm^{-1}. The peaks that are observed at 560, 868, 1353, and 1514 cm^{-1} and are assigned to fundamental modes by BZ turns out *not* to be real fundamentals. The peaks at 505, 990, and 1314 cm^{-1} are newly assigned to be real fundamentals. The remaining fundamental is predicted to be around 1128 cm^{-1}, but no peak with b_2 symmetry is found around 1128 cm^{-1}. The fundamental modes of DBT-d_8 are observed at 408, 492, 592, 670, 818, 831, 854, 965, 1017, 1040, 1293, 1338, 1381, 1542, 1564, 2000, 2270, 2283, and 2293 cm^{-1}. The peaks at 818, 965, and 1381 cm^{-1} are newly assigned to fundamentals instead of the peaks at 943, 1158, and 1355 cm^{-1}. All the fundamental modes whose frequencies are smaller than 1600 cm^{-1} consist of in-plane ring bendings, CC stretchings, and CH in-plane bendings. The other modes are CH stretchings.

C. Vibrational Frequencies of DBT in the First Triplet State. Calculated vibrational frequencies for the lowest triplet state are directly scaled by using a scaling factor of 0.963 that is recommended by RP.[18] The use of multiple scaling factors is not appropriate for this case, due to the lack of known transferable scaling factors for the excited state and the insufficient number of peaks observed in the transient Raman spectra of the excited state. The calculated and observed vibrational frequencies of only the a_1 symmetric mode for DBT in the triplet state are listed in Table 3. Included are the corresponding frequencies of DBT in the ground state, prepared in the same manner for comparison.

Buntinx and Poizat observed five bands at 977, 1079, 1330, 1445, and 1531 cm^{-1} in the transient Raman spectra of DBT. They assigned all the peaks to be fundamental modes of a_1 symmetry, based on comparisons with the vibrational frequencies of the ground state and with the assignments for the biphenyl triplet state. The peaks observed at 977, 1079, 1330, and 1445 cm^{-1} are assigned to be the 6th, 8th, 12th, and 14th a_1 fundamental modes, respectively, and are based on the comparison with the calculated frequencies for the triplet state. The vibrational frequencies of the 6th, 8th, and 14th modes of DBT in the triplet state are smaller than the corresponding ones in the ground state by 50, 58, and 35 cm^{-1}, respectively, experimentally and by 27, 38, and 27 cm^{-1}, respectively, theoretically. These modes are ascribed to the ring vibrational modes. The remaining peak observed at 1531 cm^{-1} cannot be assigned to any fundamental mode with confidence. It may be ascribed to overtones or combinations of fundamental modes of the triplet state or vibrations of other transient species. The rms deviation of the calculated frequencies from the observed ones is only about 10.7 cm^{-1} for DBT in the first triplet state. BP pointed out from their analysis of the Raman spectra that the vibrational frequencies decrease for the ring vibrational modes on going from the ground state to the triplet state and suggested, on the basis of this fact, that the geometry changes from a benzene-like to a quinone-like form upon the excitation to the triplet state. The same pattern they observed in vibrational frequencies, upon the excitation, can be seen in the calculated frequencies. Although their assignment of fundamental modes differs slightly from the present work, their suggestion about the change in the geometry upon excitation is confirmed here, as seen in section III.A.

IV. Summary

The molecular structure of dibenzothiophene in the ground and the first-excited triplet state are calculated by using the B3LYP/6-31G* method. Upon the excitation to the first triplet state, a structural change occurs from a benzene-like to a quinone-like form. The vibrational frequencies of DBT in the ground and the lowest triplet state are obtained by using a scaling procedure similar to the direct scaling method developed by Baker and co-workers. Scaled vibrational frequencies for the ground state obtained from the B3LYP calculation show good agreement with the available experimental data. Based on the calculated and the experimental vibrational frequencies, a few fundamental frequencies are newly assigned and the spectral position of missing lines are predicted.

Acknowledgment. The present research was supported by Korea Science and Engineering Foundation, KOSEF, 981-0306-033-01 1998.

References and Notes

(1) Marchand-Geneste, N.; Lacoste, C.; Budzinski, H.; Carpy, A. *Polycyclic Aromat. Compd.* **2000**, *19*, 37.
(2) Stewart, S. D.; Fredericks, P. M. *J. Raman Spectrosc.* **1995**, *26*, 629.
(3) Sander, M.; Kirsch, G. *Z. Naturforsch.* **1989**, *44a*, 205.
(4) Radziszewski, J. G.; Michl, J. *J. Am. Chem. Soc.* **1986**, *108*, 3289.
(5) Bree, A.; Zwarich, R. *Spectrochim. Acta* **1971**, *27A*, 621.
(6) Schaffrin, R.; Trotter, J. *J. Chem. Soc. A* **1970**, 1561.
(7) Barckholtz, C.; Barckholtz, T. A.; Hadad, C. M. *J. Am. Chem. Soc.* **1999**, *121*, 491.
(8) Corradi, E.; Lazzeretti, P.; Taddei, F. *Mol. Phys.* **1973**, *26*, 41.
(9) Bree, A.; Zwarich, R. *Spectrochim. Acta* **1971**, *27A*, 599.
(10) Terada, T.; Koyanagi, M.; Kandz, Y. *Bull. Chem. Soc. Jpn.* **1980**, *53*, 352.
(11) Buntinx, B.; Poizat, O. *Laser Chem.* **1990**, *10*, 333.
(12) Handy, N. C.; Maslen, P. E.; Amos, R. D.; Andrews, J. S.; Murray, C. W.; Laming, G. *Chem. Phys. Lett.* **1992**, *197*, 506.
(13) Handy, N. C.; Murray, C. W.; Amos, R. D. *J. Phys. Chem.* **1993**, *97*, 4392.
(14) Johnson, B. G.; Gill, P. M. W.; Pople, J. A. *J. Chem. Phys.* **1993**, *98*, 5612.
(15) Stephens, P. J.; Devlin, F. J.; Chavalowski, C. F.; Frisch, M. J. *J. Phys. Chem.* **1994**, *98*, 11623.
(16) Devlin, F. J.; Finley, J. W.; Stephens, P. J.; Frisch, M. J. *J. Phys. Chem.* **1995**, *99*, 16883.
(17) Wheeless, C. J. M.; Zou, X.; Liu, R. *J. Phys. Chem.* **1995**, *99*, 12488.
(18) Rauhut, G.; Pulay, P. *J. Phys. Chem.* **1995**, *99*, 3093.
(19) Lee, S. Y.; Boo, B. H. *J. Phys. Chem.* **1996**, *100*, 8782.
(20) Lee, S. Y.; Boo, B. H. *J. Phys. Chem.* **1996**, *100*, 15073.
(21) Lee, S. Y.; Boo, B. H. *Bull. Korean Chem. Soc.* **1996**, *17*, 760.
(22) Lee, S. Y. *Bull. Korean Chem. Soc.* **1998**, *19*, 93.
(23) Lee, S. Y.; Boo, B. H. *Bull. Korean Chem. Soc.* **1996**, *17*, 754.
(24) Koch, W.; Holthausen, M. C. *A Chemist's Guide to Density Functional Theory;* Wiley-VCH: Weinheim York, 2000.
(25) Baker, J.; Jarzecki, A. A.; Pulay, P. *J. Phys. Chem. A* **1998**, *102*, 1412.
(26) Becke, A. D. *J. Chem. Phys.* **1993**, *98*, 5648.
(27) Frisch, M. J.; Trucks, G. W.; Schlegel, H. B.; Scuseria, G. E.; Robb, M. A.; Cheeseman, J. R.; Zakrzewski, V. G.; Montgomery, J. A., Jr.; Stratmann, R. E.; Burant, J. C.; Dapprich, S.; Millam, J. M.; Daniels, A. D.; Kudin, K. N.; Strain, M. C.; Farkas, O.; Tomasi, J.; Barone, V.; Cossi, M.; Cammi, R.; Mennucci, B.; Pomelli, C.; Adamo, C.; Clifford, S.; Ochterski, J.; Petersson, G. A.; Ayala, P. Y.; Cui, Q.; Morokuma, K.; Malick, D. K.; Rabuck, A. D.; Raghavachari, K.; Foresman, J. B.; Cioslowski, J.; Ortiz, J. V.; Stefanov, B. B.; Liu, G.; Liashenko, A.; Piskorz, P.; Komaromi, I.; Gomperts, R.; Martin, R. L.; Fox, D. J.; Keith, T.; Al-Laham, M. A.; Peng, C. Y.; Nanayakkara, A.; Gonzalez, C.; Challacombe, M.; Gill, P. M. W.; Johnson, B.; Chen, W.; Wong, M. W.; Andres, J. L.; Gonzalez, C.; Head-Gordon, M.; Replogle, E. S.; Pople, J. A. *Gaussian 98, Revision A.7*; Gaussian, Inc.: Pittsburgh, PA, 1998.
(28) Allouche, A.; Pourcin, J. *Spectrochim. Acta A* **1993**, *49*, 571.